Graphitic nanoparticles from thermal dissociation of camphor as an effective filler in polymeric coatings

Rohit Ranganathan Gaddam[a,b], Sasidhar kantheti[a], Ramanuj Narayan[a] , KVSN Raju[a]*

a.CSIR-Indian Institute of Chemical Technology, Hyderabad -500007,Andhra Pradesh, India

b. Amity Institute of Nanotechnology, Amity University, Noida 201301, India.

* Corresponding author. : E-mail addresses: kvsnraju@iict.res.in;drkvsnraju@gmail.com

We report an easy synthesis of uniformly-sized water soluble graphitic-carbon nanoparticles (CNP) from the soot obtained by the incineration of camphor. The soot was characterized by X-ray diffraction (XRD) and Raman spectroscopy which reveal the presence of graphitic domains in the obtained nanoparticle. Scanning electron microscope (SEM) images display uniformly sized CNPs of about ~50 nm. The camphoric soot was then oxidized with a piranha solution to decorate the CNP surface with a carboxyl group. This presence of carboxyl group was confirmed by the C=O stretching at 1720.17cm^{-1} in the Fourier transform-infrared spectroscopy. Following the surface treatment, CNP was reacted with diisocyanate to form amide linkages, which was exploited in the fabrication CNP-polyurethane hybrid composite material (CNP-PU). Minuscule incorporation (0.1, 0.5 wt %) of CNP into polyurethanes show a magnificent improvement in the overall thermo-mechanical properties of the CNP-PU as compared to neat polyurethane films. From the XRD analysis of CNP-PU it is evident that incorporation of CNPs enhances the crystallinity of the resultant composite. Proper dispersion of CNPs into the polyurethane matrix was noticeable in the SEM images of the composite.

1. Introduction

Carbon is a quite fascinating material owing to its chemical diversity, which makes it amongst the most targeted material for industrial applications. Amongst all the allotropes of carbon, carbon nanomaterials like carbon nanotubes, graphite and graphene are amongst the most researched ones.[1-3] Carbon nanoparticles (CNPs) particularly have attracted a greater attention due to their significant role in a variety of fields. However it falls amongst the least researched carbon material due to the lack of proper methods of preparation and purification. They are generally found as an arc generated soot, vacuum deposited films and interstellar dust.[4] CNPs find their application as a fluorescent material,[5.6] anode material in lithium ion batteries,[7,8]optical bioimaging,[9,10]micro-sensors,[11]field emission devices[12] and optical devices.[13]The incorporation of CNPs into a polymer matrix provides an opportunity to synthesize nanocomposites that can potentially challenge the most advanced materials in nature. Development of these materials is difficult because, the thermodynamic and kinetic barriers restrain the optimal dispersion of CNPs into the polymer matrix.[14]Especially, in the case of using polyurethane matrix, it is preferable to have a chemically attachable nanoparticle to the polymer than just a physical mixing. Therefore CNP's surface modification is necessary for proper dispersal of into the polyurethane matrix. Such stable incorporations into the polyurethane matrix reduces the possibility of CNP agglomeration many fold and enhance the overall property of the nanocomposite. As the nanoparticle size gets smaller, the surface to volume ratio increases which in turn leads to a domination of surface atoms behaviour than that of the interior atoms.[15-17] Therefore these surface atoms are credited to the increase in the properties of the polymeric hybrid nanocomposite material.

The current work puts forth an eco-friendly, simple and straightforward approach for the synthesis of CNPs and its respective polyurethane hybrid nanocomposites. Camphor, a natural eco-friendly hydrocarbon, is used as a precursor material for the synthesis of CNPs. Camphor ($C_{10}H_{16}O$) is a volatile, waxy, flammable, white crystalline substance, obtained from the tree *Cinnamomumcamphora.*[18]It is a bicyclic saturated terpene ketone, which exists in the optically active dextro and levo forms, and also as a racemic mixture of the two forms. Dextro-form is amongst the most naturally occurring form that occurs in the woods and leaves of camphor tree. Since camphor is a pure hydrocarbon source, its dissociation yields mostly carbon residue.

Camphor soot is non-toxic and also has been used in India for centuries in facial decoration purposes. There are previous reports on camphor based carbon nanomaterials by chemical vapour deposition, laser ablation or other methods.[19-24]For the first time we report the production of graphitic-carbon nanoparticles by the combustion of camphor. Here the uniformly sized CNPs from camphor soot were collected on polished copper plate. Then the CNPs were subjected to oxidative purification with piranha solution for the covalent modification of the surface with a carboxylic group (CNP-COOH). The piranha solution consists of a highly reactive acidic mixture of sulphuric acid (H_2SO_4) and hydrogen peroxide (H_2O_2) in the ratio of 7:3 respectively. Once carboxyl group terminated CNPs (CNP-COOH) were prepared, this was followed by 0, 0.1 and 0.5 wt% loading of modified CNPs into polyurethanes to prepare carbon nanoparticle-polyurethane hybrid nanocomposite (CNP-PU). The as prepared CNP-Pus were highly stable and possessed exceptional physico-chemical properties.

2. Experimental section

2.1. Materials

Camphor was obtained from the local market. Commercial poly tetramethyleneglycol (PTMG), 1-isocyanato-4-[(4-isocyanato cyclohexyl) methyl] cyclohexane (H_{12}-MDI), Dibutyl tin dilaurate were purchased from Sigma Aldrich. Cellosolve acetate, conc. sulphuric acid, 30% hydrogen peroxide solution was purchased from SD Fine chemicals, Mumbai. All the chemicals were used as received without any purification.

2.2. Instruments

Fourier Transform Infrared (FTIR) spectroscopy of synthesized samples was recorded by Thermo Nicolet Nexus 670 spectrometer. X-ray Diffraction (XRD) patterns for all the samples were obtained using a Siemens D-5000 X-ray diffractometer with Cu Kα radiation of wavelength 1.54. The thermogravimetric analysis (TGA) was conducted on TGA Q500 Universal TA instrument (U.K) at temperature ramp rate of 10^0C min^{-1} from 25 to 600^{o}C with a continuous N_2 flow at the rate of 30 ml min^{-1}. Raman spectra were recorded using Horiba JobinYvon Raman spectrometer with a laser excitation wavelength of 632.81nm. Transmission electron micrographs (TEMs) were recorded on a JEOL JEM-100CX electron microscope for examining the carbon nanoparticles. The changes in morphology of CNPs due to surface modification were also observed under Field emission scanning electron microscope (FESEM) using S4300 SEIN HITACHI Japan at 10 kV. The samples were coated with a thin gold layer of ~5 nm of thickness by sputtering process to make them conducting for FESEM analysis. Tensile strength and percentage elongation was measured by Universal Tensile Machine (UTM) of AGS-10kNG, Shimadzu.

2.3. Preparation and Oxidation of CNPs

5g of camphor was taken in a copper crucible, which was subjected to burning (450^{o}C) in presence of atmospheric oxygen. The soot was collected on a polished copper plate clamped above the burning camphor. The distance between the copper plate and camphor was kept at 25cm. The soot (300mg) deposited on the copper sheet was allowed to cool till room temperature. Then the CNPs were carefully scraped out with a stainless steel spatula. Following which, the obtained CNPs were refluxed with a solution of piranha (mixture of sulphuric acid (H_2SO_4) and hydrogen peroxide (H_2O_2) in the ratio of 7:3 respectively) for 5hours. The obtained solution was vacuum filtered and washed with water several times. The filter paper was dried at 60^{o}C for 24 hours. A black powder of CNP-COOH was obtained.It was found that an initial 300mg of pristine carbon nanoparticle when subjected to oxidation produces a 220 mg final oxidized product. Therefore the loss is weight is accounted to the purification steps.

2.4. Synthesis of CNP-Polyurethane hybrid nanocomposite(CNP-PU)

Calculated amount of CNP-COOH (0%, 0.1%, 0.5% with respect to total weight), H_{12}-MDI (0.98 g, 3.73 mmol) and 2.5g of cellosolve acetate were taken in a round bottom flask. The mixture was sonicated for half an hour and stirred at 60^{o}C for three hours. To the above solution, a mixture of PTMG-1000 (1g, 1 mmol) and TMP (0.15g, 1.1 mmoles, 15 weight % with respect to PTMG) dissolved in cellosolve acetate were added drop wise . The mixture was stirred at 65^{o}C for 8 hours under inert atmosphere. In all the hybrids, OH and NCO ratio was maintained as 1:1.2. After adding one drop of 5% DBTDL in MIBK as catalyst and one drop of Tegostab as surfactant, the CNP-PU hybrid films were casted on a tin foil supported over a glass plate by a manual driven square applicator, The excess NCO present in the polyurethane nanocomposite films were moisture cured at 30^{o}C and laboratory humidity conditions (25–30%) for 15 days. The supported films were extracted after amalgamation of tin and cleaning.

3. Results and discussion

3.1. Graphitic-Carbon nanoparticle

The pristine CNPs obtained from the soot were characterized by using FESEM and TEM analysis (Fig.1), which show that the particles are highly uniform in size (~ 50 nm in diameter). The FTIR spectrum of the CNP (Fig.2a) shows two peaks around 2926 and 2960cm^{-1} which corresponds to C-H stretching for sp^2 and sp^3 hybridized carbon atoms respectively. Upon oxidative treatment of the CNPs, the CNP-COOH shows an increase in crystallinity as compared to that of the as generated CNPs. X-ray Diffraction (XRD) peaks of the CNP and CNP-COOH samples reveal two prominent peaks at 25.6^{o}and 43.6^o (Fig.2b) which can be attributed to the (002) and (100) plane of hexagonal graphite Camphor consists of ten carbon atoms of which seven are associated with ring system. Burning of camphor may lead to formation of intermediate hexagonal and pentagonal radicals, which combine together forming carbon nanoparticles. The temperature generated during combustion is essential in catering the formation of CNP.[25]

A substantial change in the crystallinity of CNP-COOH as compared to the pristine CNP could be observed from the XRD graph.The pristine CNPs upon treatment with a piranha solution increases the crystallinity of CNP. The transformation can be viewed as a constructive dehydration of H_2O_2 by H_2SO_4 to form hydronium ions, bisulphate ions and atomic oxygen. This atomic oxygen allows the piranha solution to dissolve the elemental carbons. Generally the CNPs are difficult to attack chemically, because they are highly stable and their surface carbon atoms are in sp^2 hybridization with each other. However the nascent oxygen directly attaches on to the surface of CNP, forming a carbonyl group. The oxygen atom here deceptively takes an electron bonding pair from the central carbon and forms a carbonyl group, while simultaneously disrupting the bonds of the target carbon atom with one or more of its neighbours. This triggers a cascading effect where single atomic oxygen initiates disentanglement of the local bonding structure, which in turn allows the whole range of reaction to affect the carbon atoms.[26,27] Therefore bond dissociation and association occurs as an effect of piranha solution, which may perhaps be the reason for the improvement in crystallinity of CNP-COOH, which correlates with the XRD measurement. The formation of CNP-COOH was also confirmed from FTIR analysis. The presence of sharp intense peak at 1720.17cm^{-1} corresponds to –C=O stretching and a broad distinct peak around 1200 cm^{-1} corresponds to –C-O stretching in the carboxyl group. From the thermogravimetric analysis (TGA) a prominent change in thermal stability of CNP and CNP-COOHcould be observed (Fig.2c). For instance, the onset decomposition temperature (T_{ON}) of CNP and CNP-COOH are 472 and 415^{o}C respectively. Clear differences in the thermal degradation of CNP and CNP-COOH could be noticed (Table.1).

Raman spectra of disordered carbon usually comprise of two prominent bands namely D-band (D for disorder) and G-band (G for Graphite). The D-band is found around 1350cm^{-1}, which corresponds to A_{1g} symmetry of disordered graphite and also indicates the existence of nanocrystalline graphite. The G-band could be located around 1580 cm$^{-1.}$ This band is attributed to a Zone center mode of E_{2g} symmetry of single crystal graphite. The Raman spectrum displays a comparison between the as prepared CNPs and CNP-COOH (Fig.2d). The Raman spectra of CNP clearly show the D-band near 1327cm^{-1} and G-band at 1585cm^{-1}. However the D-band of acid treated CNPs showed a downward shift to 1314cm^{-1} while the G-band remains near 1585cm^{-1}. There is also a decrease in the full width at half maximum of the D-band in the CNP-COOH in comparison with the pristine CNPs. The phenomenon of shifting downwards and narrowing of D-band in CNP-COOH is an indication of decrease in the level of disorder and an increase in the graphite domain size.[28]CNP formation from camphor involves recombination of carbon bonds on the copper surface. This induces smaller graphitic domain sizes, leading to size distributions with a variety of bonding structures. These distributions of cluster with different sizes introduce a superposition of different Raman modes, which result in a broader line-width in the case of pristine CNPs (Fig.3). The integrated intensity ratio between G-peak and D-peak is inversely proportional to the grain size of graphite. The grain size of graphite calculated from the Raman spectra is 45.36 Å for CNP and 39.94Å for CNP-COOH. This results support the narrowing of the D-band and increase in the domain size.[29,30]

3.2. CNP-Polyurethane hybrid

Once the formation of CNP-COOH was confirmed, the next step was incorporation into a polyurethane matrix (Fig.4). The successful synthesis of CNP-polyurethane hybrids is confirmed on the basis of the complete absence of free –NCO peak around 2270 cm^{-1} in the FT-IR spectra (Fig.5a), which indicates complete moisture curing of the polyurethanes. The observed absorption bands (cm^{-1}) at 3050–3700 (–NH stretch), 2800–3000 (–CH stretch consisting of asymmetric –CH_3 stretch at 2957, asymmetric –CH_2 stretch at 2920, symmetric –CH_3 stretch at

2872 and symmetric $–CH_2$ stretch at 2851 cm-1), 1600–1800 (-C=O stretching of amide I), 1500–1600 (amide II stretch consisting of a mixture of peaks $\delta_{N–H}$, $\upsilon_{C–N}$ and $\upsilon_{C–C}$), 1394 (δ_{CH2}symm/assym), 1215–1350 cm^{-1} (amide III, $\upsilon_{C–N}$), 766 (amide IV due to –NH out of plane vibration) and 720 ($–CH_2$ rocking) clearly supports the formation of polyurethanes. It is also clear from Fig.5a that the C=O str of urethane segment was observed as a doublet at 1690 and 1630 cm^{-1}. The peak at 1690 cm^{-1}correspond to C=O of non hydrogen bonded urethane segments.[31] Whereas, the peak at 1630 cm^{-1} corresponds to hydrogen bonded C=O urethane segments. The FT-IR spectra therefore affirms that the intensity of the hydrogen bonded C=O region increases with the %CNP loading (Fig.5a). It is also observed that the intensity of peak at 3400cm^{-1}(N-H region of urethane) increases with CNP loading. Therefore it is clearly evident that due to hydrogen bond formation between CNP and PU matrix, the intensity of peak at 3400cm^{-1}(N-H region of urethane) and 1630 cm^{-1} (hydrogen bonded C=O str of urethane groups) increases with CNP loading. This shows that the cross-linking ability of urethanes increases with CNP loading.[32]

Three major peaks could be observed in CNP-COOH FT-IR (Fig.2a) such as 3500 cm^{-1} (O-H str), 1720 cm^{-1} (C=O str) and 1200 cm^{-1} (C-O str). After incorporation of CNP into PU matrix, these peaks are merged with polyurethane characteristic peaks such as 3500 cm^{-1} (N-H str of urethane), 1600- 1800 cm^{-1} (C=O str) and 950-1250 cm^{-1} (C-O-C str) respectively. Fig.5brepresents the XRD pattern of CNP-COOH incorporated polyurethane as compared to the neat polyurethane. A definite increase in the crystallinity of the polyurethane could be visualized with increase in the CNP-COOH content. The nanosized CNP-COOH provides large surface area due to the density of atoms on their surface and thus it is judicious to consider that the CNP-COOH could act as effective nucleating sites for polyurethane crystallization. The increased nucleating sites are likely to facilitate the polyurethane crystallization process in CNP-PU hybrid.

The TGA analysis (Fig.5c) displays the onset of thermal degradation of samples which could be correlated with increase in CNP percentile, 0.5% CNP-PU had the highest onset temperature of 262^{o}C, in comparison with the pure (238^{o}C) and 0.1% CNP (247^{o}C) incorporated hybrid (Table.2). The tensile strength (in N/mm^2) and % elongation at break for 0%, 0.1% and 0.5% CNP-PUs (from UTM analysis (Fig.5d) are 8.10, 10.07, 16.84 and 10.74, 15.9, 19.34 respectively. The improvement in thermo-mechanical properties is attributed to proper dispersion of CNPs. The CNPs owing to their size and exceptional physico-chemical properties form a highly stable cross-linked structure with the polyurethanes, thereby enhancing the overall tensile strength and thermal stability. Water contact angle measurements show an augmented hydrophobicity with increase in the CNP-COOH concentration in the nanocomposite. The contact angle of neat polyurethane is 58.96^o which rose to 82.93^o in 0.1% and 97.1^o in 0.5% CNP-PU. This shows that the carboxyl groups present on the surface of CNP-COOH are completely reacted therefore increasing the hydrophobicity of the sample (Table.3).

The CNP-COOH is highly compatible with the polyurethane and no visible agglomerations were found in the FESEM analysis of the films (Fig.6). Neat polyurethane (0% CNP-PU) has a highly smooth surface, whereas the incorporation of CNP renovates the polyurethane matrix into a coarse and splintered microstructure with many pleats. The thermal stability and tensile strength of CNP-PU improve considerably with increase in the CNP-COOH loading. The carboxyl group present on the CNP surface reacts with diisocyanate to form amide linkages. Therefore, with increase in the CNP percentage, cross-linking increases through the formation of hydrogen bonds between the amide linkages and urethane hard segments. These formed cross-linked networks along with the existence of intermingled CNP-COOH are responsible for the improvement in the thermal and mechanical properties of the CNP-PU hybrids. The effect of incorporating CNPs in the organization of polyurethane matrix could be correlated with the increase in the density of pleats with the percentage of CNP. The formation of these rough surfaces facilitates high elongation at break and tensile strength of the polyurethane film.

4. Conclusion

The current work reveals an easy synthesis method of CNPs in a substantial quantity from camphor, which is economic and eco-friendly. Hence this method of synthesis could be used to produce carbon nanoparticles in bulk. Further, the burning camphor could be utilized in energy production. As an example for the potential use of CNPs, in the present work, the obtained CNPs were oxidized and added as filler in polyurethane matrix. The polyurethane matrix showed an increased thermo-mechanical property. The prepared CNP-PU owing to its hydrophobicity, could find its use in self-cleaning coatings. However, this work presents the preliminary insight for use of CNPs; hence additional surface modifications of CNPs could open an arena for wide range of potential usage. We hope that the CNP based polyurethane-nanocomposites hybrid materials represent a new exciting direction that may open up opportunities in surface chemistry.

Acknowledgements

The present research work was supported by CSIR, India under Intel-Coat Project (CSC-0114). The authors would like to extend their thanks to the Director, CSIR- IICT for permitting the work to be carried out.

.

References

[1] A. Hirsch, *Nature materials*, 2010,**9**,868-871.

[2] H.J. Salavagione, G. Martínez and G. Ellis, *Macromolecular rapid communications* 2011, **32**, 1771-1789.

[3] Z. Yao and K.C. Tam, *Macromolecular rapid communications*, 2011, **32**, 1863-1885.

[4] G.P. Lopinski , V.I. Merkulov and J.S. Lannin, *Physical review letters* 1998,**80**, 4241.

[5] C. Zhu, J. Zhai and S. Dong, *Chemical Communications*, 2012,**48**, 9367-9369.

[6] Y. Yang, J. Cui, M. Zheng, C.Hu, S. Tan, Y. Xiao, et al. *Chemical Communications*, 2012, **48**, 380-382.

[7] Y. Yu, L. Gu, C. Wang, A. Dhanabalan, P.A. van Aken and J. Maier *Angewandte Chemie International Edition*, 2009, **48**, 6485-6489.

[8] Y. Wang, F. Su, C.D. Wood, J.Y. Lee and X.S. Zhao, *Industrial & Engineering Chemistry Research*, 2008, **47**, 2294-2300.

[9] S. Sahu, B. Behera, T.K. Maiti and S. Mohapatra, *Chemical Communications*, 2012,**48** 8835-8837.

[10] A.B. Bourlinos, R. Zbořil, J. Petr, A. Bakandritsos, M. Krysmann and E.P. Giannelis, *Chemistry of Materials*, 2011, **24**, 6-8.

[11] M.P. Siegal, W.G. Yelton, D.L. Overmyer and P.P. Provencio, *Langmuir*, 2004, **20**, 1194-1198.

[12] Y.C. Yang, J. Tang, L. Liu and S.S.Fan.*US Pat. US7635945*, 2009.

[13] D. Vincent, S. Petit and S.L. Chin, *Applied optics*, 2002; **41**, 2944-2946.

[14] S.M. Liff, N. Kumar and G.H. McKinley, *Nature materials*, 2006; 6, 76-83.

[15] H. Akita and T. Hattori, *Journal of Polymer Science Part B: Polymer Physics*, 1999; 37(3): 189-197.

[16] J.H. Chang and Y.U. An, *Journal of Polymer Science Part B: Polymer Physics,* 2002; 40, 670-677.

[17] S.A. Zavyalov, E.I. Grigoriev, A.S. Zavyalov, I.A. Misurkin, S.V. Titov and T.S. Zhuravleva. *International Journal of Nanoscience 2005*, 4,149-161.

[18] M. Kumar and Y. Ando, Diamond and related materials, 2003,**12**, 998-1002.

[19] M. Sharon, W.K. Hsu, H.W. Kroto, D.R.M. Walton, A. Kawahara and T. Ishihara, *Journal of power sources*, 2002,**104**,148-153.

[20] M. Kumar and Y. Ando, *Carbon*, 2005; **43**, 533-540.

[21] M. Kumar and Y. Ando, *Journal of Physics: Conference Series*,2007, **61**, 643.

[22] P.R. Somani, S.P. Somani and M. Umeno, *Chemical Physics Letters* 2006,**430**, 56-59.

[23] L.F. Cui, L.Hu, J.W. Choi, Cui Y. ACS Nano, 2010; **4**, 3671-3678.

[24] R. J. Andrews, C. F. Smith & A.J. Alexander, *Carbon,* 2006, **44**, 341-347.

[25] K. Mukhopadhyaya, K.M. Krishna and M. Sharon. *Carbon,*1996*,* **34***,* 251-264.

[26] D. Diemente, *J. Chem. Educ.*, 1991, **68**, 568–269.

[27] K. S.Koh, J. Chin, J. Chia & C.L. Chiang, *Micromachines*, 2012, **3**, 427-441.

[28] J. Schwan, S. Ulrich, V. Batori, H. Ehrhardt & S. R. P. Silva, *Journal of Applied Physics* 1996, **80**, 440.

[29] G. X. Chen, M. H. Hong, T. C. Chong, H. I. Elim, G. H. Ma & W. Ji, *Journal of applied physics,* 2004, **95**, 1455-1459.

[30] D. S. Knight & W. B. White *Journal of Materials Research*,1989,**4**, 385-393.

[31] K. Sasidhar, P.S. Sarath, R. Narayan & K.V.S.N Raju, *Reactive and Functional Polymers*, 2013, **73**, 1597-1605.

[32] A.K. Mishra, R.S. Mishra, R. Narayan & K.V.S.N Raju, *Progress in Organic Coatings*, 2010, **67**, 405-413.

LIST OF FIGURES

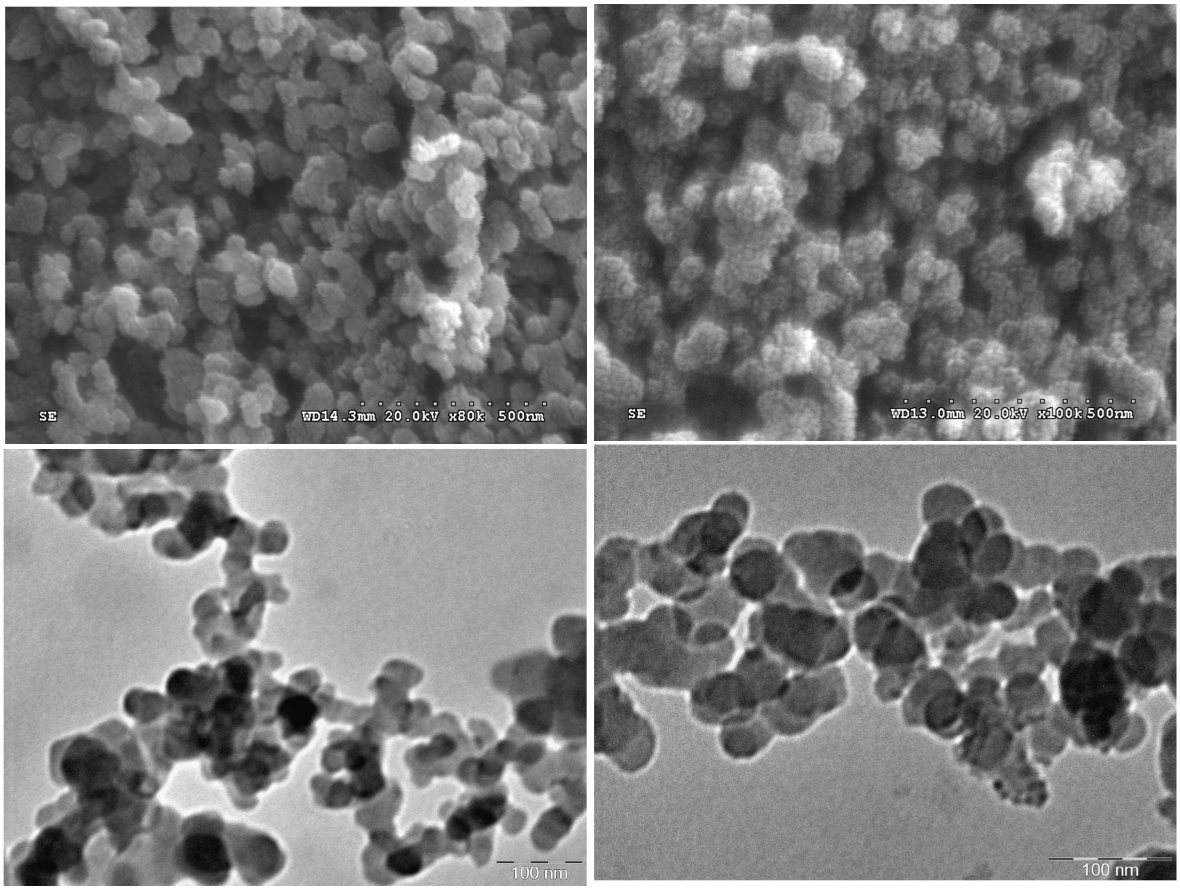

Fig. 1 FESEM images (above) and TEM images (below) of graphitic-carbon nanoparticles and piranha solution treated carbon nanoparticles (from left to right)

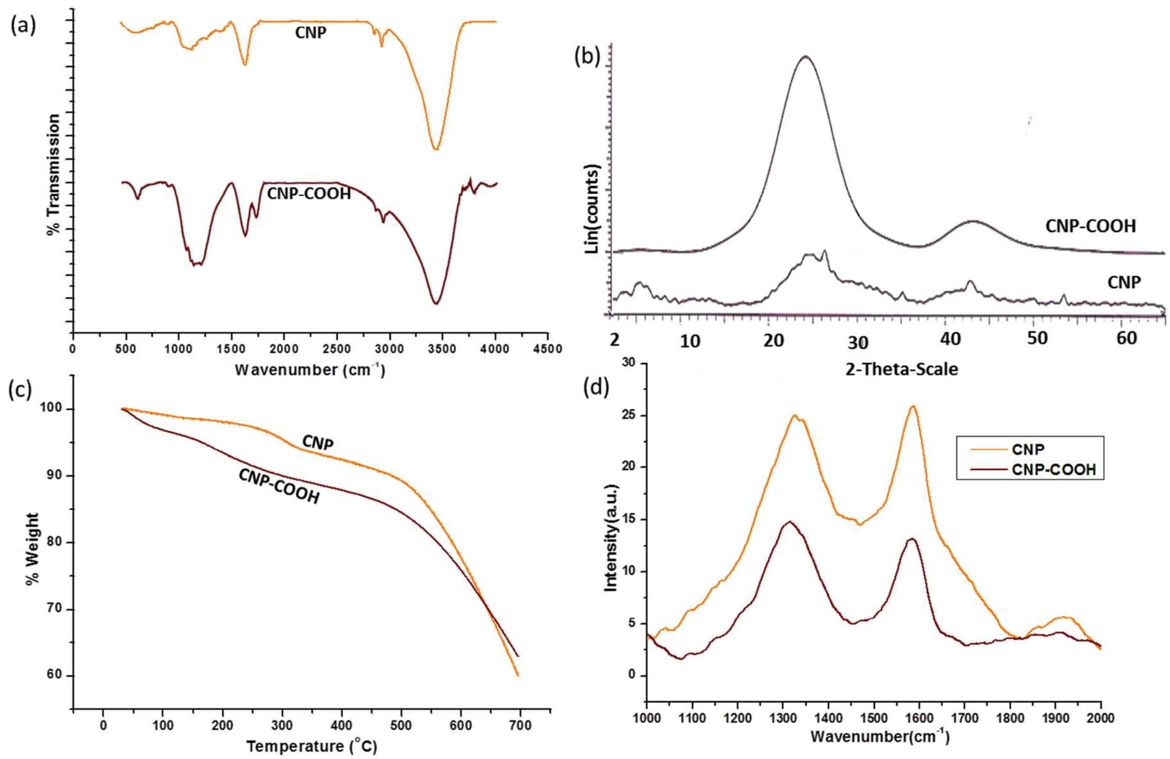

Fig. 2(a) FTIR (b) XRD graph (c) TGA graph (d) Raman analysis of CNP and CNP-COOH incorporated polyurethane.

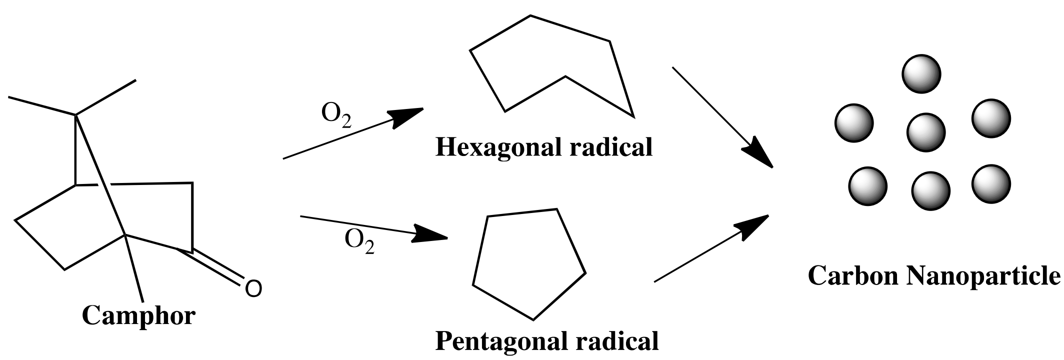

Fig. 3 Possible mechanism for the formation of carbon nanoparticles

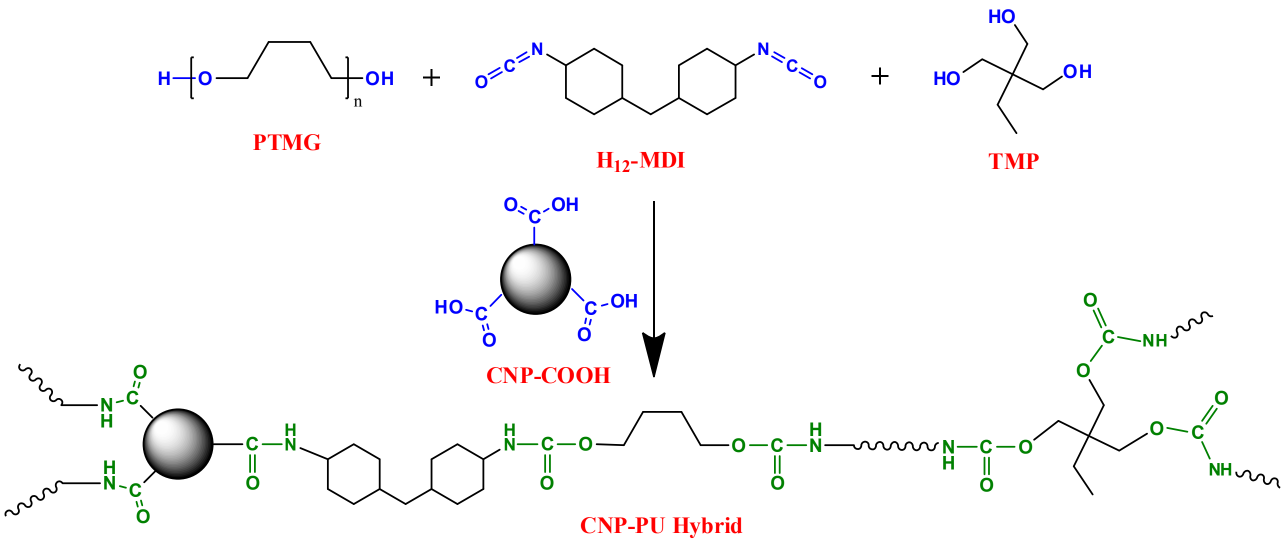

Fig.4 Reaction path for the formation of CNP-PU hybrid

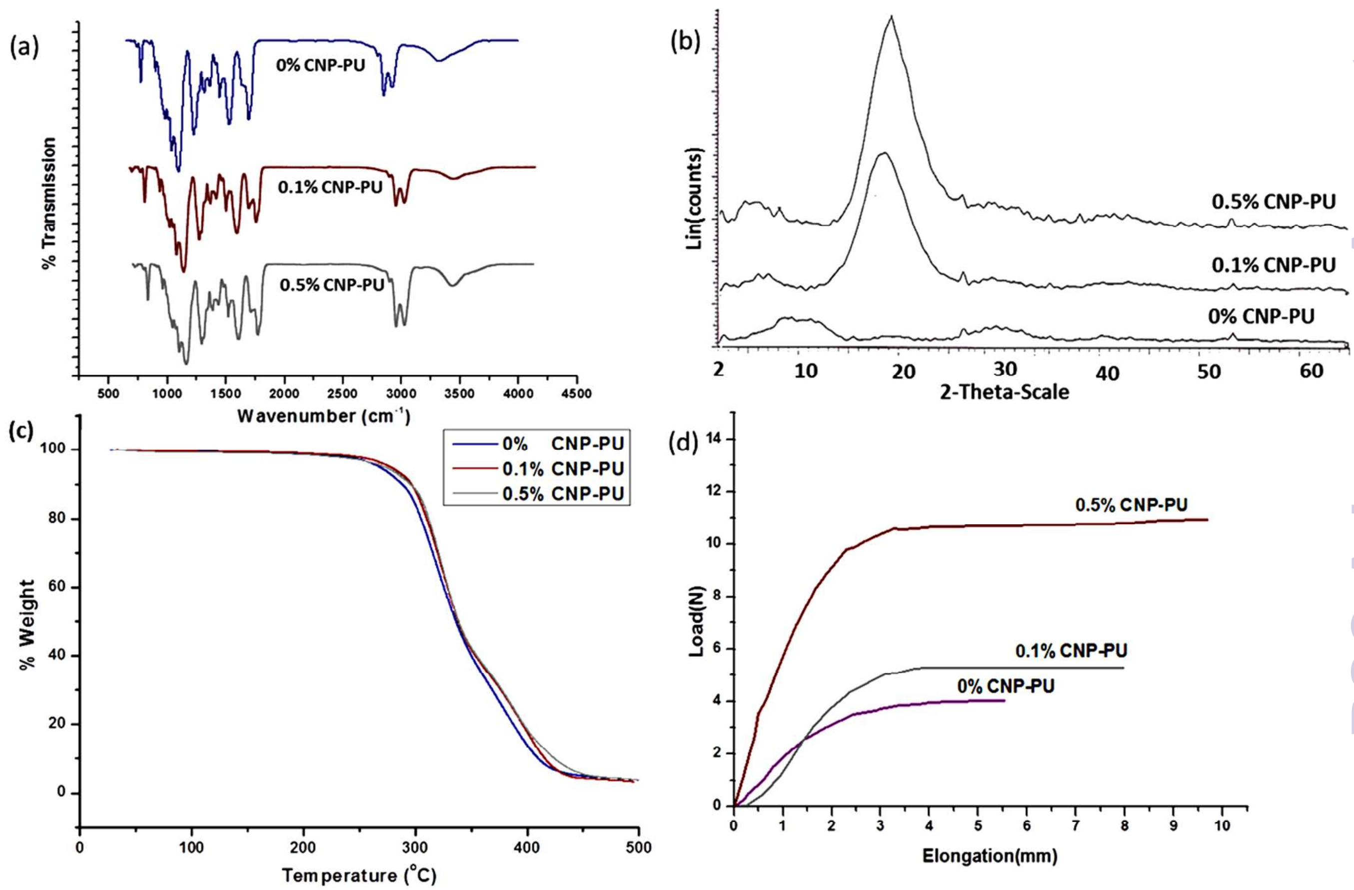

Fig. 5 (a) FTIR spectra (b) XRD graph (c) TGA analysis and (d) UTM analysis of 0%, 0.1% and 0.5% polyurethanes.

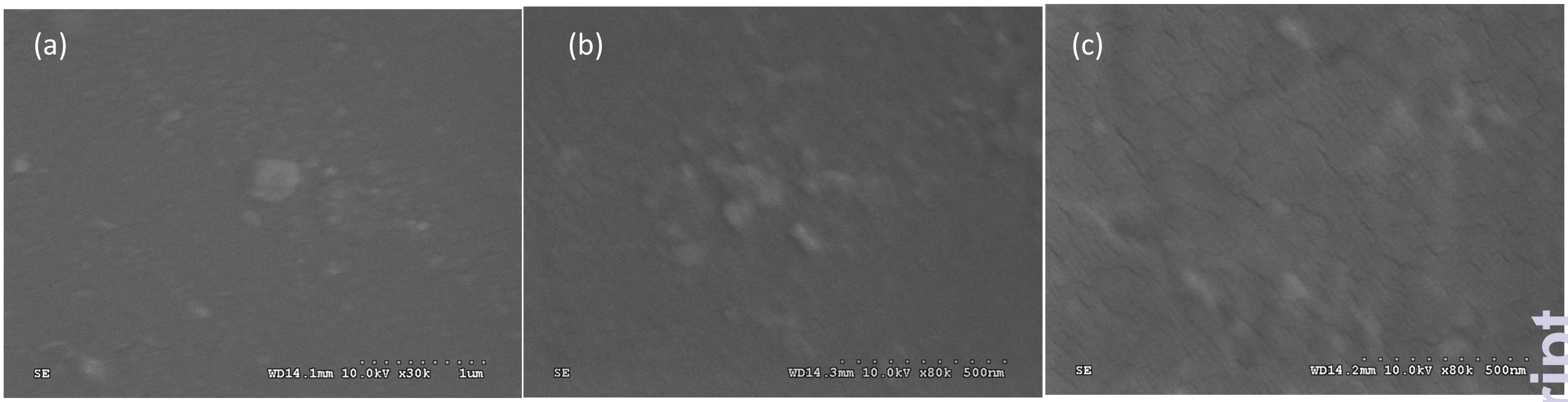

Fig.6 FESEM images of (a) Neat polyurethane (b) 0.1wt% CNP-COOH incorporated polyurethane and (c) 0.5wt% CNP-COOH incorporated polyurethane.

LIST OF TABLES

Table 1

TGA profile of various CNT samples

Sample code	Onset decomposition Temperature (T_{ON}) (°C)	10%wt loss temperature (T_{d10}) (°C)	% wt remaining at 500°C	% wt remaining at 600°C
CNP	472	482.41	89.20	77.74
CNP-COOH	415	297.84	84.51	75.91

Table 2

TGA profile of various CNT-PUs

Sample code	Onset decomposition Temperature (T_{ON}) (°C)	10%, wt loss temperature (T_{d10}) (°C)	50%, wt loss temperature (T_{d50}) (°C)	% wt remaining at 350°C	% wt remaining at400°C
0%CNP-PU	238	285.86	324.84	39.71	13.79
0.1%CNP-PU	247	294.90	328.65	41.85	17.50
0.5%CNP-PU	262	293.50	329.42	42.50	18.37

Table 3

Mechanical properties of CNT-PU hybrids

Sample code	Tensile strength (N/mm^2)	Elongation at break (%)	Water Contact angle
0%CNP-PU	8.10	10.74	58.4°
0.1%CNP-PU	10.07	15.9	82.93°
0.5%CNT-PU	16.84	19.34	97.1°

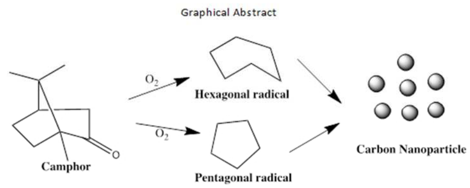

304x171mm (96 x 96 DPI)